Chapter 3

The Structures of CH_3O^- and CH_3S^- in Water Clusters

Abstract

The purpose of this chapter is to predict the geometries and charges on atoms of CH_3O^- and CH_3S^- in aqueous solution. Also, I predict the maximum number of water molecules that can directly interact with the O of CH_3O^-. For this purpose, using the ab initio closed-shell self-consistent field method with the energy gradient technique, I carried out full geometry optimizations with the MP2/aug-cc-pVDZ for $CH_3O^-(H_2O)_n$ (n = 0,1,2,3) and the MP2/6-31+G(d,p) (for n = 5,6). The structures of $CH_3S^-(H_2O)_n$ (n = 0,1,2,3) were fully optimized using MP2/6-31++G(2d,2p). It is predicted that the $CH_3O^-(H_2O)_6$ does not exist. I also performed vibrational analysis for all clusters [except $CH_3O^-(H_2O)_6$] at the optimized structures to confirm that all vibrational frequencies are real. Those clusters have all real vibrational frequencies and correspond to equilibrium structures. The results show that the above maximum number of water molecules for CH_3O^- is five in the gas phase. For $CH_3O^-(H_2O)_n$, when n becomes larger, the C-O bond length becomes longer, the C-H bond lengths become smaller, the HCO bond angles become smaller, the charge on the hydrogen of CH_3 becomes more positive, and these values of $CH_3O^-(H_2O)_n$ approach the corresponding values of CH_3OH with the n increment. The C-O bond length of $CH_3O^-(H_2O)_3$ is longer than the C-O bond length of CH_3O^- in the gas phase by 0.044 Å at the MP2/aug-cc-pVDZ level of theory. Therefore, it is predict that the structure of CH_3O^- in aqueous solution is considerably different from that in the gas phase. The structure of the CH_3S^- moiety in CH_3S^-

$(H_2O)_n$ does not change with the n increment. Thus, it is predicted that the structure of CH_3S^- in aqueous solution is almost equal to that in the gas phase.

1. Introduction

Many chemically and biologically important species exist in RO^- and RS^- in aqueous solution. Many important drugs (for example, alcohols) exist in RO^- in aqueous solution. The compounds (for example, thiols) related to the protection of DNA from radiation damage exist in RS^- in aqueous solution. However, at the present stage of experimentation, it is impossible to determine the geometries of RO^- and RS^- in aqueous solution. As the initial step in determining the geometries of RO^- and RS^- in aqueous solution, the structures of CH_3O^- and CH_3S^- in aqueous solution are interesting.

However, for CH_3O^-, only $CH_3O^-(H_2O)$ was investigated by many theoretical researchers. The acidities and deprotonation energies were calculated [1]. The geometry and energy were calculated using 6-31G(d) [2]. Calculated and experimental hydrogen bond strengths were compared [3]. The geometry and energy were calculated using 6-31+G(d) [4]. The full optimizations were performed using STO-3G, 3-21G, 6-31G(d), MP2/6-31G(d), 6-31+G(d) and MP2/6-31+G(d) [5]. Fully optimized structures, normal vibrational modes, and thermodynamic functions were obtained at the MP2/6-311++G(d,p) level [6]. A number of density functional methologies were systematically examined for their ability to describe strong hydrogen bonds [7]. Experimentally, the following were performed: The thermochemistry of the mixed water-methanol anionic clusters $[(H_2O)_n(CH_3OH)_m-H]^-$ was determined [8], the relative acidities of water and methanol were measured [9], and $CH_3O^-(H_2O)_6$ was analyzed using x-ray studies of the crystal [10]. In aqueous solution, the Monte Carlo calculation shows that five water molecules strongly bond the O of CH_3O^- in aqueous solution [4]. For $CH_3S^-(H_2O)_n$, the geometry of $CH_3S^-(H_2O)_n$ was optimized using the 6-31G(d) [2] and 6-31+G(d) basis sets [4]. The interaction energy and interatomic distances for the thiolate-one water complex were calculated using STO-3G, 3-21G, 6-31G(d), 6-31+(d), MP2/6-31G(d), MP2/6-31+G(d), PM3, and AM1 [5]. The structures and energetics of $CH_3S^-(H_2O)_n$ (n = 1— 4) were calculated using ROHF/6-31G(d) [11]. Experimentally, $\Delta H^0_{n-1,n}$ for $CH_3S^-(H_2O)_n$ (n = 1,2,3,4) were measured [12]. In aqueous solution, the Monte Carlo calculation shows that six water molecules strongly bond the S of CH_3S^- [4].

The purpose of this chapter is to predict the geometries and charges on atoms of CH_3O^- and CH_3S^- in aqueous solution. Also, I predict the maximum number of water molecules that can directly interact with the O of CH_3O^-.

2. Method

Using the ab initio closed-shell self-consistent field (SCF) method with the energy gradient technique, I carried out full geometry optimization with the MP2/aug-cc-pVDZ for $CH_3O^-(H_2O)_n$ (n = 0,1,2,3) and CH_3OH in Fig. 1. The frozen core was used. In general, MP2/aug-cc-pVDZ is reliable for such systems. $CH_3O^-(H_2O)_n$ (n $\geq$ 4) was not fully optimized with MP2/aug-cc-pVDZ because of a huge amount of CPU time. Therefore, to predict the above maximum number of water molecules, the structures of $CH_3O^-(H_2O)_n$ (n = 5,6) were fully optimized using MP2/6-31+G(d,p).

For $CH_3S^-(H_2O)_n$, the structures were fully optimized using MP2/6-31++G(2d,2p) (for n = 0,1,2,3). $CH_3S^-(H_2O)_n$ (n $\geq$ 4) were not fully optimized using MP2/6-31++G(2d,2p) because of the huge amount of CPU time necessary.

I also performed vibrational analysis for all clusters at the optimized structures to confirm that all vibrational frequencies are real.

The energies were calculated using MP2/aug-cc-pVDZ for $CH_3O^-(H_2O)_n$ and MP2/6-31++G(2d,2p) for $CH_3S^-(H_2O)_n$. The energy changes ($\Delta E_{n-1,n}$) of

$$CH_3O^-(H_2O)_{n-1} + H_2O \longrightarrow CH_3O^-(H_2O)_n$$

were calculated by the following formula:

$$\Delta E_{n-1,n} = E(CH_3O^-(H_2O)_n) - E(CH_3O^-(H_2O)_{n-1}) - E(H_2O)$$

The enthalpy changes ($\Delta H^{298K}{}_{n-1,n}$) were also calculated by a similar formula, and basis set superposition error (BSSE) was also corrected using the counterpoise method [13].

$$\Delta H^{298K} = \Delta E_e{}^o + \Delta E_v{}^o + \Delta(\Delta E_v{}^{298K}) + \Delta E_r{}^{298K} + \Delta E_t{}^{298K} + \Delta(PV),$$

where $\Delta E_e{}^o$ is the electronic energy change, $\Delta E_v{}^o$ is the change in the zero-point energy, $\Delta(\Delta E_v{}^{298K})$ is the change in the vibrational energy on going to 298K, and the remaining quantities are for the changes in rotational and translational energy and the work term that were treated classically. Similar calculations were performed for $CH_3S^-(H_2O)_n$.

For the evaluation of the reliability of MP2/aug-cc-pVDZ, the following calculations were performed: (1) Because the proton affinity difference between CH_3O^- and OH^- is important, the proton affinity difference evaluated by MP2/aug-cc-pVDZ was compared with the experimentally determined proton affinity difference and (2) the enthalpy changes ($\Delta H^{298K}_{n-1,n}$) in MP2/aug-cc-pVDZ were compared with the experimental $\Delta H^0_{n-1,n}$. Similar comparisons were made for $CH_3S^-(H_2O)_n$.

For the analysis of atomic electron populations, the natural population analysis was used [14].

I used the Gaussian 94 [15] and Gaussian 98 [16] programs and the SP2, HSP, HPC, and SX-5 computers at the Institute for Molecular Science. I also used the Gaussian 94 program and SP2 computer in the Computer Center of Tokyo Metropolitan University.

3. Results

All clusters [except $CH_3O^-(H_2O)_6$] have all real vibrational frequencies and correspond to equilibrium structures.

CH_3O^-

The proton affinity difference evaluated by MP2/aug-cc-pVDZ (ΔE = 7.4 kcal/mol) is close to the experimentally determined proton affinity difference (ΔH = 9.5 kcal/mol) [9].

Table 1 shows the $-\Delta H^{298K}_{n-1,n}$ in MP2/aug-cc-pVDZ to be equal to the experimental $-\Delta H^0_{n-1,n}$ [8]. The counterpoise corrected values are worse than the uncorrected values, which agrees with Ref. [17]. This is true for $CH_3S^-(H_2O)_n$. Table 2 shows literature data for $-\triangle E$ and $-\triangle H$ in $CH_3O^-(H_2O)$. Our results agree with MP2/6-31+G(d) and MP2/6-311++G(d,p) calculations and experimental data.

Fig. 1 shows the structures. There are some similarities between the $CH_3O^-(H_2O)_n$ and $OH^-(H_2O)_n$ (n = 2,3,4) [18]. The following findings are true for $CH_3S^-(H_2O)_n$.

1. $CH_3O^-(H_2O)$: H_4-C_2-O_1...H_6-O_7-H_8 nealy forms a plane. (In the MP2/aug-cc-pVDZ, the $H_6O_1C_2H_4$ torsional angle is 7.3°, the $O_7H_6O_1$ bond angle is 182.3°, and the $H_8O_7H_6O_1$ torsional angle is -16.3°).

2. $CH_3O^-(H_2O)_n$ (n = 2,3,4): The hydrogen bond between water molecules exists. The hydrogen bonds between water molecules are important factor for forming clusters.

$CH_3O^-(H_2O)_6$ does not exist because the sixth water molecule invariably migrated to the second solvent shell during the optimization, leading to a structure best represented as $CH_3O^-(H_2O)_5(H_2O)$.

Table 3 and 4 show the changes in structural parameters and charges on the atoms in $CH_3O^-(H_2O)_n$ with each n increment. When n becomes larger, the C-O bond length becomes longer, the C-H bond lengths become smaller, the HCO bond angles become smaller, the charge on the hydrogen of CH_3 becomes more positive, and these values of $CH_3O^-(H_2O)_n$ approach the corresponding values of CH_3OH with the n increment.

For the C-O bond length of $CH_3O^-(H_2O)$, our result disagree with 6-31G(d) and 6-31G(d)+P calculations.

CH_3S^-

The proton affinity difference evaluated by MP2/6-31++G(2d,2p) (ΔE = 33.1 kcal/mol) is nearly equal to the experimentally determined proton affinity difference (ΔH = 34.5 kcal/mol) [19].

Table 5 shows that $-\Delta H^{298K}_{n-1,n}$ in MP2/6-31++G(2d,2p) is equal to the experimental $-\Delta H^{0}_{n-1,n}$ [12]. Table 2 shows that our result is better than the MP2/6-31+G(d) calculation.

Fig. 2 shows the structures. Table 6 and 7 show that the structure of CH_3S^- moiety in the $CH_3S^-(H_2O)_n$ structure does not depend on the number of n.

Discussion

CH_3O^-

It is predicted that the cause for the shortening of the C-O bond in CH_3O^- in the gas phase is negative hyperconjugation (H^- CH_2=O) [20]. Because the C-O bond length of $CH_3O^-(H_2O)_n$ becomes longer with each n increment, it is predicted that the negative hyperconjugation decreases with the n increment. The C-O bond length of $CH_3O^-(H_2O)_3$ is 0.044 Å longer than the C-O bond length of CH_3O^- in the gas phase. Therefore, it is predicted that the structure of CH_3O^- in aqueous solution is considerably different from that in the gas phase.

The results show that the maximum number of water molecules that can directly interact with the O of CH_3O^- is five in the gas phase. It is noteworthy that five water molecules strongly bond to the O of CH_3O^- in aqueous solution using the Monte Carlo calculation.

CH_3S^-

The characteristics of $CH_3S^-(H_2O)_n$ are different from those of $CH_3O^-(H_2O)_n$. Because the C-S bond length of $CH_3S^-(H_2O)_n$ is close to that of CH_3SH, it is predicted that the negative hyperconjugation (H^- SH_2=O) does not exist in the CH_3S^- moiety of $CH_3S^-(H_2O)_n$. Because the structure of CH_3S^- moiety in the $CH_3S^-(H_2O)_n$ structure does not change with the n increment, it is predicted that the structure of CH_3S^- in aqueous solution is almost equal to that in the gas phase.

Appendix

Full optimized structural parameters are available from author (free of charge).

References

[1] S.Ikuta, J.Comput.Chem. 4(1984)374.

[2] J.Gao, D.S.Garner and W.L.Jorgensen, J.Am.Chem.Soc. 108(1986)4784.

[3] I.H.Williams, J.Am.Che.Soc. 109(1987)6299.

[4] W.L.Jorgensen and J.M.Briggs, J.Am.Chem.Soc. 111(1989)4190.

[5] Ya-J.Zheng and K.M.Merz Jr., J.Comp.Chem. 9(1992)1151.

[6] A.T.Pudzianowski, J.Chem.Phys. 102(1995)8029.

[7] A.T.Pudzianowski, J.Phys.Chem.,100(1996)4781.

[8] M.Meot-Ner (Mautner), J.Am.Chem.Soc. 108(1986)6189.

[9] M.Meot-Ner (Mautner) and L.W.Sieck, J.Phys.Chem. 90(1986)6687).

[10] A.Bino, J.Am.Chem.Soc. 109(1987)275.

[11] Anny-O.Colson and M.D.Sevilla, J,Phys.Chem. 98(1994)10484.

[12] L.W.Sieck and M.Meot-Ner (Mautner). J.Phys.Chem. 93(1989)1586.

[13] S.F.Boys and F.Bernardi, Mol.Phys. 19(1970)553.

[14] A.E.Reed, R.B.Weinstock and F.Weinhold, J.Chem.Phys. 83(1985)735.

[15] M.J.Frisch, G.W.Trucks, H.B.Schlegel, P.M.W.Gill, B.G.Johnson, M.A.Robb, J.R.Cheeseman, T.Keith, G.A.Petersson, J.A.Montgomery, K.Raghavachari, M.A.Al-Laham, V.G.Zakrzewski, J.W.Ortiz, J.B.Foresman, J.Cioslowski, B.B.Stefanov, A.Nanayakkara, M.Challacombe, C.Y.Peng, P.Y.Ayala, W.Chen, W.M.Wong, J.L.Andres, E.S.Replogle, R.Gomperts, R.L.Martin,

D.J.Fox, J.S.Binkley, D.J.Defrees, J.Baker, J.P.Stewart, M.Head-Gordon, C.Gonzalez, and J.A.Pople, Gaussian 94, Gaussian, Inc., Pittsburgh PA, 1995.

[16] M.J.Frisch, G.W.Trucks, H.B.Schlegel, G.E.Scuseria, M.A.Robb, J.R.Cheeseman, V.G.Zakrzewski, J.A.Montgomery, Jr., R.E.Stratmann, J.C.Burant, S.Dapprich, J.M.Millam, A.D.Daniels, K.N.Kudin, M.C.Strain, O.Farkas, J.Tomasi, V.Barone, M.Cossi, R.Cammi, B.Mennucci, C.Pomelli, C.Adamo, S.Clifford, J.Ochterski, G.A.Petersson, P.Y.Ayala, Q.Cui, K.Morokuma, D.K.Malick, A.D.Rabuck, K.Raghavachari, J.B.Foresman, J.Cioslowski, J.V.Ortiz, B.B.Stefanov, G.Liu, A.Liashenko,P.Piskorz,I.Komaromi, R.Gomperts, R.L.Martin, D.J.Fox, T.Keith, M.A.Al-Laham, C.Y.Peng, A.Nanayakkara, C.Gonzalez,M.Challacombe, P.M.W.Gill, B.Johnson, W.Chen, M.W.Wong, J.L.Andres, C.Gonzalez, M.Head-Gordon, E.S.Replogle, and J.A.Pople, Gaussian 98, Gaussian, Inc., Pittsburgh PA, 1998.

[17] E.R.Davidson and S.J.Chakravorty, Chem.Phys.Lett. 217(1994)48.

[18] M.Masamura, THEOCHEM, in press.

[19] J.E.Bartmess, R.T.McIver, in: M.T.Bowers (Ed.) Gas Phase Ion Chemistry, Academic Press, New York, 1979, pp.87-121.

[20] K.B.Wiberg, J.Am.Chem.Soc.112(1990)3379.

Table 1

Enthalpy change ($-\Delta H^{298K}_{n-1,n}$) for $CH_3O^-(H_2O)_n$ cluster with MP2/aug-cc-pVDZ

	MP2/aug-cc-pVDZ			Experiment[a]
n	E_t[b] (hartree)	$-\Delta E_{n-1,n}$ (kcal/mol)	$-\Delta H^{298k}_{n-1,n}$ (kcal/mol)	$-\Delta H^0_{n-1,n}$ (kcal/mol)
CH_3OH	-115.42193			
0	-114.80626			
1	-191.10758	25.4	24.4 (22.3)[c]	23.9
2	-267.40249	21.3	19.3 (17.3)	19.2
3	-343.69355	18.9	16.8 (14.7)	14.8

[a]Ref. [8].

[b]$E(H_2O)$ = -76.26091.

[c]BSSE corrected value.

Table 2

Literature data for $CH_3O^-(H_2O)$ and $CH_3S^-(H_2O)$ (kcal/mol)

Cluster	Reference	Basis set	-△E	-△H
$CH_3O^-(H_2O)$	1	6-31(d)	25.2	
		6-311(d)	23.7	
		6-311G(d,p)+p	21.7	
		[5s4p1d/3s1p]	22.3	
	2	6-31G(d)	25.4	
		6-31+G(d)	21.8	
		MP2/6-31+G(d)	25.4	
	3	3-21G	37.2	
		MP2/6-31G(d)	29.7	
	4	6-31+G(d)	20.4	
	5	MP2/6-31+G(d)	26.4	24.3
	6	MP2/6-311++G(d,p)		24.7
	7	MP2/6-311++G(d,P)	26.0	
		B3-LYP/6-311++G(d,p)	25.1	
		B-LYP/6-311++G(d,p)	24.3	
		B-LYP/6-31++G(d,p)	25.2	
		B-LYP/6-31+G(d,p)	25.9	
		B-LYP/TZVP+	25.7	
		B-LYP/TZVP	27.9	
		B-LYP/DNPP	28.0	
	This study	MP2/aug-cc-pVDZ	25.4	24.4
		MP2/6-31++G(d)	26.3	24.8

	Experiment			23.9
$CH_3S^-(H_2O)$	4	6-31+G(d)	11.6	
	5	MP2/6-31+G(d)	17.1	13.0
	This study	MP2/6-31++G(2d,2p)	16.1	14.8
	Experiment			15.0

Table 3

MP2/aug-cc-pVDZ Optimized Structure of $CH_3O^-(H_2O)_n$ Cluster[a]

n	C-O	C-H	HCO
0	1.361	1.138	115.1
1	1.383	1.124	113.6
	(1.333)	(1.117)	(115.2)[b]
	(1.348)	(1.110)	(114.3)[c]
	(1.330)[d]		
2	1.395	1.118	112.7
3	1.405	1.114	112.1
CH_3OH	1.435	1.101	110.0

[a]The values are mean values. Bond lengths are in angstroms, and the bond angles are in degrees.

[b]6-31G(d) calculation [1].

[c]6-31G(d)+P calculation [1].

[d]6-31G(d) calculation [2].

Table 4

Charges on Atoms of $CH_3O^-(H_2O)_n$ Cluster Using MP2/aug-cc-pVDZ

n	O_1	C_2	H_3	H_4	H_5
0	-1.019	-0.177	0.065	0.065	0.065
1	-0.973	-0.195	0.098	0.114	0.098
2	-0.962	-0.205	0.128	0.127	0.115
3	-0.960	-0.211	0.138	0.138	0.138
CH_3OH	-0.770	-0.223	0.188	0.167	0.167

Table 5

Enthalpy Change ($-\Delta H^{298K}_{n-1,n}$) for $CH_3S^-(H_2O)_n$ Cluster with MP2/6-31++G(2d,2p)

	MP2/6-31++G(2d,2p)			Experiment[a]
n	E_t[b] (hartree)	$-\Delta E_{n-1,n}$ (kcal/mol)	$-\Delta H^{298k}_{n-1,n}$ (kcal/mol)	$-\Delta H^0_{n-1,n}$ (kcal/mol)
CH_3SH	-438.02396			
0	-437.44745			
1	-513.73688	16.1	14.8 (13.1)[c]	15.0
		(14.3)[d]	(12.8)[e]	
2	-590.02389	14.6	13.2 (11.8)	13.5
		(12.9)	(12.1)	
3	-666.31080	14.5	11.8 (9.8)	11.1
		(11.8)	(11.2)	

[a]Ref. [12].

[b]$E(H_2O)$ = -76.26379.

[c]BSSE corrected value.

[d]6-31G(d) calculation [11].

[e]6-31+G(d) calculation [11].

Table 6

MP2/6-31++G(2d,2p) Optimized Structure of $CH_3S^-(H_2O)_n$ Cluster[a]

n	C-S	C-H	HCS
0	1.842	1.094	111.7
1	1.842	1.093	111.3
2	1.842	1.092	111.0
3	1.834	1.091	110.9
CH_3SH	1.826	1.086	109.5

[a]The values are mean values. Bond lengths are in angstroms, and the bond angles are in degrees.

Table 7

Charges on Atoms of $CH_3S^-(H_2O)_n$ Cluster Using MP2/6-31++G(2d,2p)

n	S_1	C_2	H_3	H_4	H_5
0	-0.756	-0.784	0.180	0.180	0.180
1	-0.698	-0.779	0.186	0.193	0.187
2	-0.692	-0.776	0.198	0.200	0.192
3	-0.733	-0.764	0.197	0.197	0.197
CH_3SH	-0.039	-0.782	0.238	0.231	0.231

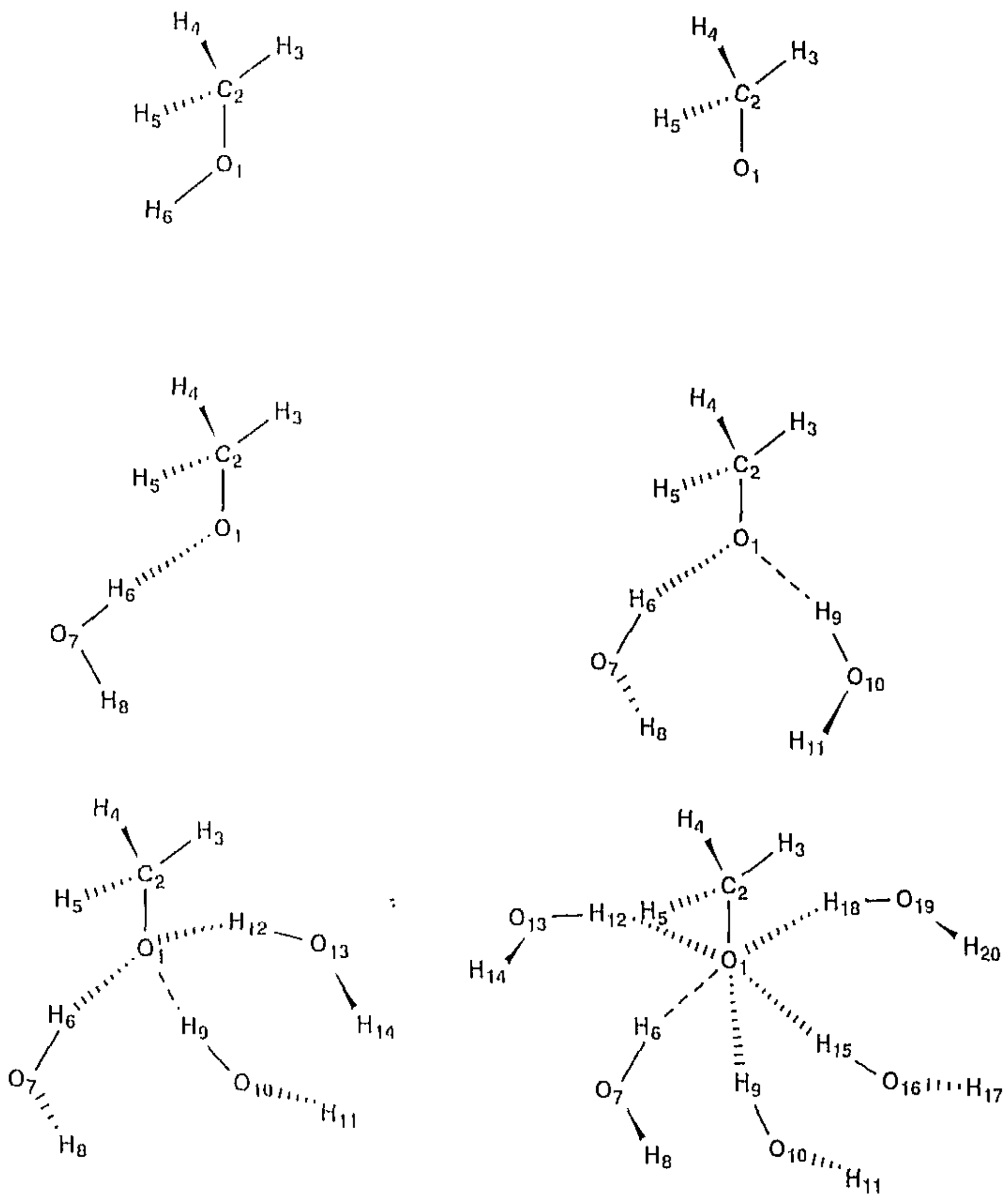

Fig. 1. The structures of $CH_3O^-(H_2O)_n$ clusters and CH_3OH.

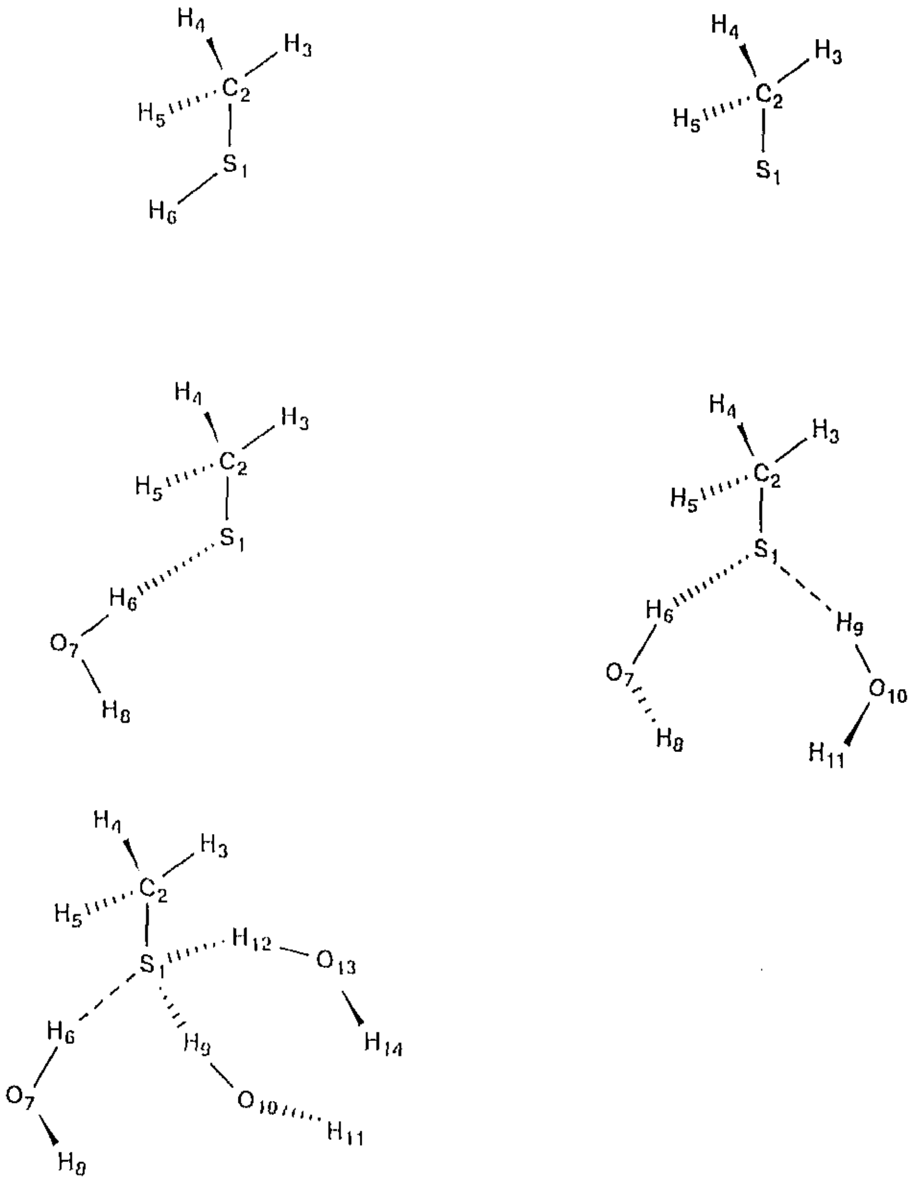

Fig. 2. The structures of $CH_3S^-(H_2O)_n$ clusters and CH_3SH.